

Detecting Energy Emissions from a Rotating Black Hole

Maurice H. P. M. van Putten^{1*} and Amir Levinson²

The rotational energy of a black hole surrounded by a torus is released through several channels. We have determined that a minor fraction of the energy is released in baryon-poor outflows from a differentially rotating open magnetic flux tube, and a major fraction of about $\eta/2$ is released in gravitational radiation by the torus with angular velocity $\eta \sim 0.2$ to 0.5 relative to that of the black hole. We associate the energy emitted in baryon-poor outflows with gamma-ray bursts. The remaining fraction is released in torus winds, thermal emissions, and (conceivably) megaelectron-volt neutrino emissions. The emitted gravitational radiation can be detected by gravitational wave experiments and provides a method for identifying Kerr black holes in the Universe.

Gravitation is a universal force in nature, and it ultimately leads to black holes as fundamental objects. Supermassive black holes are believed to form the nuclei of galaxies (1), and stellar-mass black hole candidates are found in soft x-ray transients (2) and galactic microquasars (3). Rotating black holes, discovered by Kerr as exact solutions to general relativity (4), are of great astrophysical interest because their emissions provide a method for identifying and studying black holes. Kerr black holes build up angular momentum, and this energy can be emitted in accord with the Rayleigh criterion and the first law of thermodynamics. Spontaneous emissions in vacuo are suppressed by canonical angular momentum barriers (5), but Kerr black holes—surrounded by a torus magnetosphere supported by surrounding matter—do not behave in this way. Frame-dragging on magnetic flux tubes introduces potential drops by Faraday induction, which, in the limit of superstrong magnetic fields, may suppress these barriers to allow spontaneous emission of electrons and positrons at gamma-ray burst luminosities, with an associated electromagnetic radiation (6).

A Kerr space-time has three properties: (i) Its horizon surface is compact, like those of nonrotating Schwarzschild black holes. The radius of this surface is proportional to the mass of the object. It causally separates the interior of the black hole from its surrounding environment. (ii) It exhibits frame-dragging, a general relativistic effect that causes physical objects to be dragged into orbital motion with respect to distant stars by the black hole rotation (7). (iii) It has a compact reservoir of rotational energy, which can be parameterized as $E_{\text{rot}} = 2M \sin^2(\lambda/4)$ in terms of $\sin \lambda = a/M$, the ratio of specific angular momentum $a = J_H/M$ to the

black hole mass M . A maximally rotating black hole thus stores about half of its rotational energy in the top 10% of its angular velocity $\Omega_H = \tan(\lambda/2)/2M$. Here, we describe a strategy to identify Kerr black holes from emissions in the electromagnetic and gravitational wave spectrum. Black hole emissions will be processed simultaneously along the axis of rotation and through the surrounding matter. Kerr black holes, therefore, can be identified from additional fractions of rotational energy emitted into these two channels and their compactness beyond the neutron star limit.

We consider a system consisting of a Kerr black hole surrounded by a magnetized torus (Figs. 1 and 2). It exhibits a topology similar to a pulsar magnetosphere, with a coaxial structure of open magnetic flux tubes. The inner flux tube extends from the horizon of the black hole (with ingoing radiative boundary conditions) to

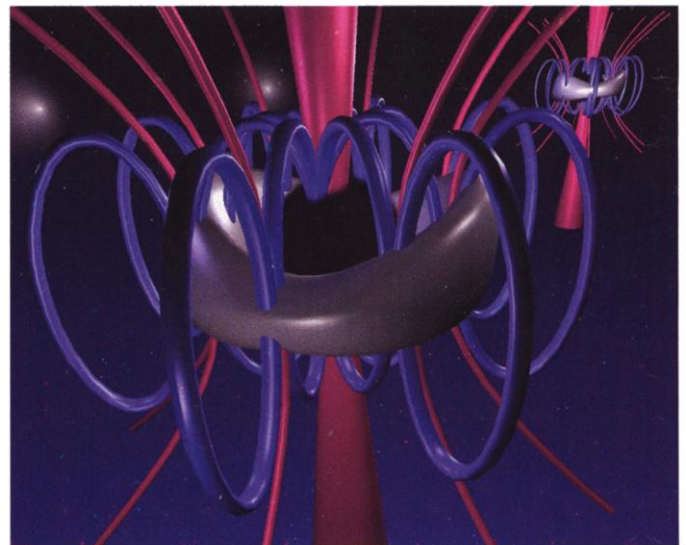
infinity (with outgoing radiative boundary conditions). It thereby satisfies slip boundary conditions on the horizon and at infinity. The outer flux tube is anchored to the torus and corotates with it. A black hole surrounded by a magnetized torus assumes a lowest energy state with a magnetic moment given by

$$\mu_H^e \approx aB_p J_H \quad (1)$$

(8), where B_p denotes the mean of the poloidal magnetic field in the surrounding torus magnetosphere. This magnetic moment corresponds to the Wald equilibrium charge q (9) and is a consequence of the no-hair theorem (8, 10, 11); the torus has a charge of opposite sign by equivalence to pulsars (12). Equation 1 holds in the force-free limit (13, 14), so that the black hole maintains a maximal and uniform magnetic flux at the horizon at arbitrary rotation rates.

The open flux tube supported by μ_H^e of Eq. 1 may serve as an artery for black hole spin energy in a manner somewhat analogous to the Penrose process. Indeed, it has been shown (15) that the total specific energy of magnetohydrodynamic inflow becomes negative when certain conditions are satisfied—in particular when $0 < \Omega_+ < \Omega_H$ (where Ω_+ is the angular velocity of magnetic field lines threading the horizon)—thereby giving rise to an outward flow of energy. The mechanism that creates the open coaxial flux tube is not understood. It could be due to a fast magnetosonic wave in the surrounding torus magnetosphere, perhaps initiated by superradiance (16), thereby accompanied by an outer flux tube supported by the inner face of the torus with magnetic flux of equal magnitude

Fig. 1. Artist's impression of a black hole-torus system in a state of suspended accretion. The black hole supports an open magnetic flux tube (red) by a magnetic moment $\mu_H^e \approx aB_p J_H$ in equilibrium with the surrounding torus magnetosphere. It forms an artery for the spin energy of the black hole, producing baryon-poor outflows as input to GRBs by dissipation due to differential frame-dragging. The torus forms a catalytic converter of black hole spin energy by equivalence in poloidal topology to pulsar magnetospheres (blue magnetic field-lines on the inner face of the torus). In a state of suspended accretion, the torus reradiates this input into various channels, including gravitational radiation, Poynting flux-dominated winds (red magnetic field-lines on the other face of the torus), thermal emissions, and (conceivably) neutrino emissions. The gravitational radiation is emitted by a quadrupole moment in the torus as a result of a mass inhomogeneity of about 0.15% relative to the mass of the black hole (30).



¹Massachusetts Institute of Technology, Room 2-378, Cambridge, MA 02139, USA. ²School of Physics and Astronomy, Tel Aviv University, Tel Aviv 69978, Israel.

*To whom correspondence should be addressed. E-mail: mvp@schauder.mit.edu

and opposite sign. We emphasize that the formation of the coaxial flux tube structure envisioned here involves processes different from dragging of magnetic field lines by magnetohydrodynamical wind ejecta. In terms of a vector potential A_ϕ , the flux in the inner tube is $+2\pi A_\phi$ and the flux in the outer tube is $-2\pi A_\phi$.

The charge density ρ_e exhibits a polarization cone (in poloidal cross section) about the torus similar to that in pulsars (17) and a bifurcation in the charge density along the inner flux tube. The charge density about the axis of rotation of the black hole satisfies $\rho_e = -(\Omega + \beta)B/2\pi$, where Ω now denotes the angular velocity of the flux tube, which may vary along the axis of rotation, and β is the frame-dragging angular velocity (1). A sign change from positive (in a lower section attached to the black hole) to negative (in the semi-infinite section above) occurs at some height above the black hole when $0 < \Omega < \Omega_H$. This permits a continuous flow of electric current along the open flux tube from infinity into the black hole, with outflow of excess negative charges to infinity and inflow of excess positive charges into the black hole. Beyond the critical points of the inflow and outflow, the four-current (a contravariant tensor j^b of electric current) becomes asymptotically null ($j^2 = 0$), consistent with a wave impedance of an open wave guide. For a net magnetic flux of $2\pi A_\phi$, it can be shown formally that in the small-angle approximation the lower section of the inner tube carries a current $I_+ \approx -(\Omega_H - \Omega_+)A_\phi$ into the horizon (18),

whereas the outflow in the upper section carries a current $I_- \approx -\Omega_- A_\phi$ from infinity (8) (where Ω_- is the angular velocity of the upper section). Charge conservation ($I_+ = I_-$) then implies that in general $\Omega_+ - \Omega_- \neq 0$, as stated above. This differential rotation induces a potential drop $\Delta V = (\Omega_+ - \Omega_-)A_\phi$ along the inner magnetic flux tube (Fig. 3).

The inner tube mediates Poynting fluxes (19) $S_\pm = E_{R\pm}B_\phi/4\pi = \Omega_\pm^2 A_\phi^2/\pi R^2$ near the horizon and at infinity, where E_R is the radial component of the electric field and B_ϕ is the azimuthal component of the magnetic field (in cylindrical coordinates). Assuming a uniform current density across the inner tube, the associated power is

$$P_j = \int (S_+ - S_-)2\pi R dR = -I\Delta V/2 \quad (2)$$

This dissipation energy constitutes a minor fraction of the black hole spin energy, given by

$$\frac{E_j}{E_{\text{rot}}} \approx \eta \left(\frac{1 - 2\eta}{1 - \eta} \right) \left(\frac{\theta_H^2}{2} \right)^2 \quad (3)$$

where $\eta = \Omega_-/\Omega_H < 1/2$ for an open flux tube with half-opening angle θ_H on the horizon. Here, we have converted the outflow luminosities of (20) to output energies over the duration of suspended accretion. Under the above assumption that there are no transverse currents, global current closure should take place over the outer flux tube that is corotat-

ing with the torus. The corresponding one-sided poloidal current flowing in the outer flux tube is given by $I_T = \Omega_T A_\phi$ on either side of the equatorial plane. The total power carried by these outflows is $\Omega_T^2 A_\phi^2$. Current closure, $I_T + I_- = 0$, then implies $\Omega_- = \Omega_T$ and hence $\eta = \Omega_T/\Omega_H$.

The differentially rotating gap between the upper and lower sections of the inner magnetic flux tube also serves as a plasma source that replenishes the particles lost from the inner tube. This is accomplished through generation of electron-positron pairs by curvature photons, emitted by the charged particles in their motion along curved magnetic field lines. Because the component of the electric field \mathbf{E} along the magnetic field \mathbf{B} does not vanish in the gap, a test particle will instantaneously accelerate to a terminal Lorentz factor at which curvature drag balances the Lorentz force. For a curvature radius $\rho = 10^6 \rho_6$ cm (where ρ_6 denotes the radius in units of 10^6 cm), the energy of a curvature photon is

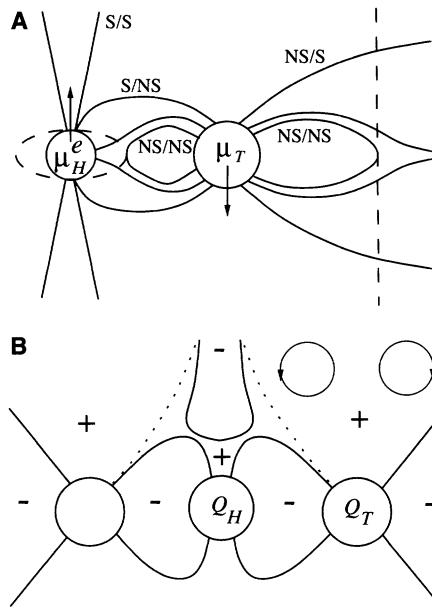
$$\epsilon_\gamma = 1.5\Gamma^3 \hbar c/\rho = 10^{-10.5}\Gamma^3/\rho_6 \text{ eV} \quad (4)$$

where Γ is the average Lorentz factor of the charged particles, \hbar is Planck's constant divided by 2π , and c is the velocity of light. The pair production threshold, $\epsilon_\gamma = 2m_e c^2$ in terms of the electron mass m_e , then implies that $\Gamma > \Gamma_c \approx 10^{5.5}\rho_6^{1/3}$ is required for pair creation to ensue. We find that the interaction length of particles having Γ just above the threshold is much smaller than the gap size, and so catastrophic pair production would ensue once Γ sufficiently exceeds Γ_c . Because the potential drop along magnetic field lines in the gap is imposed by external conditions, the component of \mathbf{E} parallel to \mathbf{B} cannot be screened out by charge separation in the gap, as envisioned in the case of pulsar inner gaps (21). Consequently, the Lorentz factors of the charged particles should be maintained near Γ_c , so that the average pair creation rate is just about equal to their escape rate. Collective effects and radiative backreaction may further play an important role in the process of plasma production. The resulting bulk Lorentz factor of the emerging outflow may turn out to be smaller than Γ_c .

Because $\mathbf{E} \cdot \mathbf{B} \neq 0$, charged particles experience a transverse drift. Consequently, their streamlines may diverge radially outward. We therefore expect the fluid to accumulate near the boundary separating the inner and outer flux tubes, where $\mathbf{E} \cdot \mathbf{B}$ approaches zero. This may require some external support of the inner tube. A plausible scenario for support is confinement of the outflow by the ram pressure of a baryon-rich wind (22) or, at larger distances, static pressure from the external medium.

The ratio of magnetic to kinetic energy in

Fig. 2. (A) The B topology of the magnetic field in poloidal cross section of a black hole–torus system. The torus is endowed with a magnetic moment density μ_T . The inner and outer face of the torus each support a torus magnetosphere that is equivalent to that of a pulsar, wherein the horizon of the black hole is identified with infinity. The black hole supports an open magnetic flux tube by its equilibrium magnetic moment $\mu_H^e \approx aB_{j_H}$ in the external poloidal magnetic field B , where $a = J_H/M$ denotes the specific angular momentum of the black hole with mass M and angular momentum J_H . The labels S and NS respectively denote slip and no-slip boundary conditions on a magnetic field line. The dashed lines delimit inner and outer bags of last closed field lines attached to the torus with no-slip/no-slip boundary conditions. [Reprinted from (8) with permission from Elsevier Science.] **(B)** The charge distribution of a black hole–torus system in poloidal cross section. The equilibrium charge separation is described by positive and negative charges separated by curves of zero charge density (solid lines). Along the axis of rotation, the charge distribution around a Kerr black hole constitutes a bifurcation from that around a Schwarzschild black hole, whose zero charge density curves are indicated by the dotted lines. The circulation patterns of Faraday-induced electric currents between the inner face of the torus and the black hole, and between the outer face of the torus and infinity, are indicated by the two circles with counterclockwise and clockwise orientations, respectively. The equilibrium charge Q_H of the black hole generates the magnetic moment (7). The torus has a corresponding equilibrium charge Q_T with opposite sign, analogous to that on a pulsar (12).



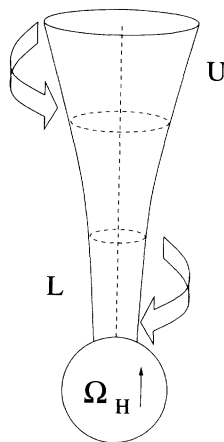
the expelled outflow is

$$\sigma = \frac{S_-}{S_+ - S_-} \approx \frac{\Omega_T}{\Omega_H - 2\Omega_T} \quad (5)$$

which, for a rapidly rotating black hole, is of order unity because $0.2 < \Omega_T/\Omega_H < 0.5$ for a canonical range $2 < R/M < 4$ of the radius of the torus around an extreme Kerr black hole. Consequently, for these parameters a differentially rotating gap is an efficient converter of electromagnetic energy into kinetic energy. The regime where $\Omega_H \leq 2\Omega_T$ is not considered here, in part because it represents black holes with modest rotational energy. A fraction of the outflow energy is carried by MeV photons associated with the aforementioned pair creation threshold. We therefore predict that this class of transient sources should exhibit prodigious high-energy emission. Further analysis is required to determine the properties of the emitted spectrum. For instance, additional dissipation of the bulk energy of the outflow may occur beyond the gap by interactions with baryon-rich material (e.g., a confining wind that can lead to oblique shocks).

Here we propose that these low- σ output energies E_j given by Eqs. 3 and 5 represent the baryon-poor input to cosmological gamma-ray bursts (GRBs). GRBs are characteristically nonthermal emissions in the range of a few hundred keV, with a bimodal distribution in durations of short bursts around 0.3 s and long

Fig. 3. An open flux tube along the axis of rotation contains upper (U) and lower (L) sections with angular velocities Ω_- and Ω_+ , in view of the slip/slip boundary conditions at infinity and on the horizon of the black hole. In the limit of supercritical ideal magnetohydrodynamics, flows out to infinity and into the black hole have current four-vectors satisfying $j^2 \rightarrow 0$. The currents mediated by the upper and lower sections within A_ϕ (= constant) become $I_- = -\Omega_- A_\phi$ and $I_+ = -(\Omega_H - \Omega_+) A_\phi$ (in the small-angle approximation), where Ω_- and $-(\Omega_H - \Omega_+)$ denote the angular velocities as seen by an observer with local zero angular momentum, as indicated by the large arrows with opposite orientation. In the present sign convention, this corresponds to retrograde rotation in the lower section. Current continuity $I_- = I_+$ with no cross-currents between neighboring flux tubes implies differential rotation between the upper and lower sections. This results in a Faraday-induced potential difference $\Delta V = (\Omega_- - \Omega_+) A_\phi$ across a gap between the two sections. Global current closure is an outer flux tube supported by and in corotation with the torus, whose magnetic flux is $-2\pi A_\phi$ (not shown).



bursts around 30 s (23). Black hole plus disk or black hole–torus systems are believed to be a canonical outcome of high angular momentum progenitors, notably in failed supernovae (24), hypernovae (25), or black hole–neutron star coalescence (26), where the former is connected to star-forming regions (25, 27). The recently inferred true GRB energy is $E_\gamma \approx 3 \times 10^{50}$ to 5×10^{50} ergs (28). In our model, the energies E_j represent a minor fraction $E_j/E_{\text{rot}} \approx 10^{-4}/\epsilon$ of the rotational energy of the black hole for $M = 7 M_\odot$, where $\epsilon \sim 0.15$ may serve as a fiducial value for the radiative efficiency of GRBs. By Eq. 3, the open flux tubes have $\theta_H \approx 35^\circ$, which provides a natural limit for the observed opening angles θ_j on the celestial sphere (20). This depends only weakly on $M \approx 3$ to $14 M_\odot$, ϵ , and η .

The inner and outer face of the torus are each equivalent to a pulsar magnetosphere as seen in a frame of reference fixed, respectively, to the horizon and infinity (Mach principle). When the black hole spins rapidly, the inner face of the torus receives energy and angular momentum, as does a pulsar when infinity wraps itself around the star with the same relative angular velocity $\Omega_H - \Omega_T$ (16, 29, 30). The outer face always loses energy and angular momentum, as does a pulsar in flat space-time with angular velocity Ω_T . The state of suspended accretion exists for the lifetime of rapid spin of the black hole (29). This equivalence to pulsars indicates a high incidence of the black hole luminosity onto the inner face of the torus. The torus thereby forms an efficient catalytic converter of the spin energy of the black hole. The torus is thus expected to become luminous in gravitational radiation, Poynting flux–dominated winds, thermal emissions, and, when sufficiently hot, megaelectron-volt emissions. Its energetic output in gravitational radiation may reach a major fraction

$$E_{\text{gw}}/E_{\text{rot}} \approx \eta/2 \quad (6)$$

of the rotational energy of the black hole, in terms of the ratio of black hole–to–torus angular velocities η (31, 32); that is, the gravitational wave energy E_{gw} reaches a few percent of M and is some two orders of magnitude larger than E_j for canonical values of θ_H .

The output E_{gw} in gravitational waves emitted by the torus may be detected by the upcoming broadband gravitational wave observatories LIGO (33) and VIRGO (34). This offers a potential test for the existence of Kerr black holes: Events for which the inferred compactness satisfies

$$2\pi \int_0^{E_{\text{gw}}} f dE > 0.005 c^5/G \quad (7)$$

(31)—where f is the frequency in gravitational waves, and G is Newton's constant—cannot be produced by rapidly spinning neutron stars (30). We expect a positive correlation

between $T/(1+z)$ and E_{gw} set by the luminosity of the black hole into the inner face of the torus. This follows from $E_j \propto E_{\text{rot}} \propto M$ and a black hole–torus coupling proportional to M^{-1} for a universal poloidal magnetic energy/kinetic energy ratio in the torus (29).

A future distribution of durations of LIGO/VIRGO detections of the predicted gravitational wave emissions is expected to be consistent with the currently known distribution of redshift-corrected durations of GRBs. Including a beaming factor of about 500 and strong cosmological evolution, the local event rate is estimated to be about one event per year with a distance of 100 Mpc (28); if the GRB rate per comoving volume is roughly constant, the same beaming factor would imply a much higher event rate. Identification of bright orphan radio afterglows that emerge several months after the GRB event could be used to search for the proposed gravitational wave emissions in future LIGO/VIRGO archive data.

References and Notes

1. D. Lynden-Bell, *Nature* **223**, 690 (1969).
2. C. D. Bailyn et al., *Astrophys. J.* **499**, 367 (1998).
3. I. F. Mirabel, L. F. Rodríguez, *Nature* **371**, 46 (1994).
4. R. P. Kerr, *Phys. Rev. Lett.* **11**, 237 (1963).
5. W. G. Unruh, *Phys. Rev. D* **10**, 3194 (1974).
6. M. H. P. M. van Putten, *Phys. Rev. Lett.* **84**, 3752 (2000).
7. In this rotating frame, which is characterized by an angular velocity $d\phi/dt = -\beta$, a physical observer assumes a state of zero angular momentum. This angular velocity equals the hole angular velocity Ω_H on the horizon, and decreases with distance from the hole to zero at infinity.
8. M. H. P. M. van Putten, *Phys. Rep.* **345**, 1 (2001).
9. R. M. Wald, *Phys. Rev. D* **10**, 1680 (1974).
10. B. Carter, *Phys. Rev.* **174**, 1559 (1968).
11. The no-hair theorem states that black holes are parameterized by mass M , angular momentum J_H , and electric charge q , with no further detailed structure. As a consequence, the horizon charge q assumes the angular velocity Ω_H and generates a magnetic moment $\mu_H = qJ_H/M$ (10).
12. J. M. Cohen, L. S. Kegeles, A. Rosenblum, *Astrophys. J.* **201**, 783 (1975).
13. The force-free condition is defined by neglecting Reynolds stresses in ideal magnetohydrodynamics. In particular, it implies vanishing of the electric field component along the magnetic field: $\mathbf{E} \cdot \mathbf{B} = 0$. On the horizon, this gives rise to a positive normal component of the electric field $E_n = -E_\phi B_\phi/B_n$, commensurate with $\mu_H > 0$. Minimizing the electrostatic energy $\mathcal{E} \approx 1/2 C q^2 - \mu_H B$ gives Eq. 1, where $C \approx 1/M$ denotes the capacitance of the black hole.
14. H. K. Lee, C. H. Lee, M. H. P. M. van Putten, *Mon. Not. R. Astron. Soc.* **324**, 731 (2001).
15. A. Takahashi et al., *Astrophys. J.* **363**, 206 (1990).
16. M. H. P. M. van Putten, *Science* **284**, 115 (1999).
17. P. Goldreich, W. H. Julian, *Astrophys. J.* **157**, 869 (1969).
18. B. Punsly, F. Coroniti, *Astrophys. J.* **350**, 518 (1990).
19. Poynting flux describes the transport of electromagnetic energy defined by $\mathbf{S} = [1/(4\pi)] \mathbf{E} \times \mathbf{B}$.
20. M. H. P. M. van Putten, A. Levinson, *Astrophys. J.* **555**, L41 (2001).
21. M. A. Ruderman, P. G. Sutherland, *Astrophys. J.* **196**, 51 (1975).
22. A. Levinson, D. Eichler, *Phys. Rev. Lett.* **85**, 236 (2000).
23. C. Kouveliotou et al., *Astrophys. J.* **413**, L101 (1993).
24. S. E. Woosley, *Astrophys. J.* **405**, 273 (1993).
25. B. P. Paczynski, *Astrophys. J.* **494**, L45 (1998).

26. ———, *Acta Astron.* **41**; 257 (1991).
 27. J. S. Bloom, S. R. Kulkarni, S. G. Djorgovski, *Astrophys. J.*, in press; available at <http://xxx.lanl.gov/abs/astro-ph/0010176> (2000).
 28. D. A. Frail *et al.*, *Astrophys. J.* **562**, L55 (2001).
 29. M. H. P. M. van Putten, E. C. Ostriker, *Astrophys. J.* **552**, L31 (2001).
 30. M. H. P. M. van Putten, *Astrophys. J.* **562**, L51 (2001).
 31. ———, *Phys. Rev. Lett.* **87**, 0901101 (2001).
 32. Gravitational radiation in the suspended accretion state (31) is described by a fraction $L_{\text{gw}}/L_H \approx \alpha/(\alpha + f_w^2)$ of the luminosity L_H of the black hole produced by a quadrupole moment in the torus with angular velocity $\Omega_r/\Omega_H \approx f_H^2/(\alpha + f_H^2 + f_w^2)$, where $\alpha \approx 3 - 2f_w^2$, and f_H and f_w are the fractions of magnetic flux supported by the torus associated with the inner torus magnetosphere around the black hole and the torus wind to infinity, respectively. Equation 6 uses $L_{\text{gw}}/L_H \approx 0.5$; (31) gives a more conservative estimate.
 33. A. Abramovici *et al.*, *Science* **256**, 325 (1992).
 34. C. Bradaschia *et al.*, *Phys. Lett. A* **163**, 15 (1992).

35. Supported by NASA grant 5-7012, an MIT C. E. Reed award, and a NATO collaborative linkage grant. We thank P. F. A. M. van Putten for providing Fig. 1. M.v.P. thanks R. Weiss and P. L. Fortini for stimulating discussions.

4 December 2001; accepted 5 February 2002
 Published online 21 February 2002;
 10.1126/science.1068634
 Include this information when citing this paper.

Spontaneous Air-Driven Separation in Vertically Vibrated Fine Granular Mixtures

N. Burtally, P. J. King,* Michael R. Swift

We report the observation of the spontaneous separation of vertically vibrated mixtures of fine bronze and glass spheres of similar diameters. At low frequencies and at sufficient vibrational amplitudes, a sharp boundary forms between a lower region of glass and an upper region of the heavier bronze. The boundary undergoes various oscillations, including periodic tilting motion, but remains extremely sharp. At higher frequencies, the bronze separates as a mid-height layer between upper and lower glass regions, and the oscillations are largely absent. The mechanism responsible for the separation can be traced to the effect of air on the granular motion.

Granular materials occur widely in nature, and the ability to handle grains and powders is central to numerous industrial processes (1, 2). The dynamics of large grains is controlled by the inelastic collisions between grains and with constraining surfaces (3); under vibration the grains may exhibit flow (4), convection (5, 6), arching (7, 8), and the formation of striped, square, or hexagonal patterns (9, 10). The “Brazil nut effect,” in which a larger grain moves to the top of a collection of smaller grains (11), is also well known.

Since the time of Faraday, air has been known to strongly influence the motion of fine particulates (12), leading to the spontaneous formation of heaps in vertically vibrated granular layers (12, 13) and to the spontaneous tilting of collections of fine grains vibrated vertically within a box (14). Recently it has been reported that air also has an influence on the Brazil nut effect (15). However, to date, there is no general consensus on the basic mechanism responsible for these air-driven effects (15–18). Similarly, there is now a substantial body of knowledge on segregation and separation in granular composites (19), but a clear understanding of many of the physical processes involved is still lacking (20–24). Furthermore, much of the attention has been focused on large particulate systems where air effects do not play a major role.

We report investigations of the behavior of mixtures of fine particles when subjected to vertical vibration in the presence of air, carried out to explore the interplay between granular separation and the influence of air on the motion. We restrict ourselves to describing the surprising separation behavior exhibited by a fine binary mixture having components with very similar properties save for their densities. The effect represents a novel ordering mechanism in vibrated granular materials in the presence of a surrounding fluid. This phenomenon, being distinct from size segregation, clearly has important implications for the mineral extraction, pharmaceutical, and powder processing industries, where the separation of fine particulates of equal sizes has been notoriously difficult.

Initially we consider a mixture consisting of bronze spheres of density 8900 kg/m³ and of diameters spanning the range 90 to 120 μm, mixed with glass spheres of density 2500 kg/m³ and of the same 90 to 120 μm size range, in the proportion 25%:75% by volume. The dynamic angles of repose are 23.4° ± 0.5° and 23.9° ± 0.5° for the glass and bronze spheres, respectively, and measurements in vacuum indicate that, at low impact velocities, the coefficients of normal restitution are both very close to unity. The mixture, of mean depth 20 mm, is contained in a glass box 50 mm high and of internal dimensions 40 mm by 10 mm in the horizontal plane. The box is attached to an electromechanical transducer that is used to induce vertical sinusoidal motion, with the axis of the trans-

ducer and the sides of the box aligned to the vertical to within 1°. The resulting motion is monitored by accelerometers attached to the box. The vertical vibration may conveniently be characterized by a parameter $\Gamma = A\omega^2/g$, where A is the amplitude of the oscillation, $\omega = 2\pi f$ is the angular frequency, and Γ is the ratio of the maximum acceleration of the box to the acceleration due to gravity, g . At higher values of Γ , some static attraction between the glass spheres and the walls of the box occurs. A trace of antistatic agent is added as an aid to photography; this is observed not to affect the separation phenomena that we now report.

We have studied the behavior between $\Gamma = 1$ and $\Gamma = 20$ and over the frequency range from $f = 10$ Hz to $f = 170$ Hz. Figure 1 indicates the regions of the f - Γ plane where the various effects are observed. Once Γ slightly exceeds unity, relative motion of the grains occurs. For all frequencies, there is a low- Γ

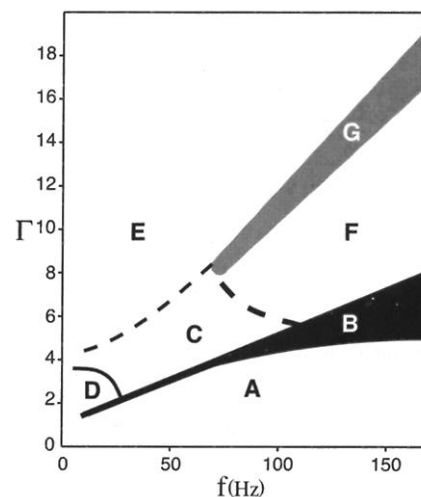


Fig. 1. Schematic diagram showing the various phenomena found at different conditions of Γ and f . Region A: region of convection and weak separation. Region B: the lower limit indicates appearance of sharp separation boundaries; the upper limit indicates almost complete separation into bronze-rich and glass-rich phases. Regions C and D: regions of oscillation of the upper surface and separation boundaries. Region D: region of simple tilt oscillations. Region E: region of intense throwing of the upper grains. Region F: region of bronze sandwiched between upper and lower glass domains. Region G: high-frequency region where inversion occurs and the bronze layer moves to a lower level.

School of Physics and Astronomy, University of Nottingham, Nottingham NG7 2RD, UK.

*To whom correspondence should be addressed: E-mail: p.j.king@nottingham.ac.uk